Geophysical Research Letters

RESEARCH LETTER
10.1029/2019GL083383

Intensification of the Pre-Meiyu Rainband in the Late 21st Century

John C. H. Chiang[1], Johannes Fischer[2], Wenwen Kong[1], and Michael J. Herman[1]

[1]Department of Geography, University of California, Berkeley, CA, USA, [2]Institute of Meteorology, University of Hamburg, Hamburg, Germany

Key Points:
- Late 21st century intensification of pre-Meiyu rainband results from enhanced meridional stationary eddy circulation over East Asia
- Enhanced eddy circulation coincides with increased westerlies impinging on Tibetan Plateau from warmer tropical tropospheric temperature
- Suggests a first-order role for westerlies in the East Asian summer rainfall response to future global warming

Supporting Information:
- Supporting Information S1

Correspondence to:
J. C. H. Chiang,
jch_chiang@berkeley.edu

Citation:
Chiang, J. C. H., Fischer, J., Kong, W., & Herman, M. J. (2019). Intensification of the pre-Meiyu rainband in the late 21**st** century. *Geophysical Research Letters*, *46*, 7536–7545. https://doi.org/10.1029/2019GL083383

Received 19 APR 2019
Accepted 6 JUN 2019
Accepted article online 17 JUN 2019
Published online 1 JUL 2019

Abstract Increased atmospheric moisture content and changing land-ocean thermal contrasts are usually implicated in the East Asian summer rainfall response to global warming. We highlight an additional influence whereby increased meridional stationary eddy circulation downstream of the Tibetan Plateau drives a stronger moisture flux convergence over southeastern China, intensifying the early summer rainband. This effect occurs robustly across the Community Earth System Model large ensemble Representative Control Pathway 8.5 simulations, and only for its pre-Meiyu stage (mid-May through late June). The westerly jet impinging on the Plateau is also enhanced, suggesting an orographic influence on the westerlies as the root cause. The increased westerlies result from warmer tropical tropospheric temperatures that enhance the meridional temperature gradient at the latitudes of the Plateau. Our results highlight the potential role of the westerlies in altering the East Asian early summer monsoon rainfall in the late 21st century.

Plain Language Summary Early summer rainfall over East Asia is projected to increase in the future as consequence of two related physical changes resulting from global warming: more moisture in the air with warmer temperatures, and stronger monsoonal circulations. A set of state-of-the-art simulations of the future climate that we analyzed suggests that the rainfall increase will be especially pronounced in the "pre-Meiyu" stage (mid-May to late June) when the East Asian rainband extends from southeastern China to southern Japan; at the end of the century, rainfall over southeastern China is projected to increase up to 40%. The cause of this intensification is different: it occurs because the westerlies "linger" at the latitudes of the Tibetan Plateau during this time instead of migrating northward, and the resulting atmospheric flow downstream brings about stronger convergent flows that concentrates and delivers more moisture to the pre-Meiyu rainband. More work, and using other models, will be needed to demonstrate that this future pre-Meiyu intensification is real. However, the significance of our result from a climate science viewpoint is in demonstrating that the change in the westerlies impinging on the Tibetan Plateau can have a first-order effect on future changes to the East Asian summer rainfall climate.

1. Introduction

Summer rainfall over the East Asian monsoon region increases in response to future greenhouse warming (Kitoh et al., 2013; Zou & Zhou, 2013). Attribution to specific mechanisms points to the thermodynamic effect of increasing specific humidity under warming (Chen & Bordoni, 2016; Held & Soden, 2006) and also to the increasing land-ocean contrast between eastern Asia and the western North Pacific and associated circulations (Kamae et al., 2014). Recent studies split the land-sea contrast response to global warming into "fast" and "slow" components whereby the fast warming over land leads to a stronger Asian monsoon cyclone and North Pacific anticyclone, but the slower ocean warming counters the circulation induced by the initial enhanced land-ocean contrast (Shaw & Voigt, 2015). Chen and Bordoni (2016) found this to be the case for an early summer enhancement of the East Asian monsoon rainband in the multimodel Coupled Model Intercomparison Project phase 5 (CMIP5) 4xCO_2 simulations.

There is also emerging interest in the role of the Tibetan Plateau on the formation of the East Asian climate and its changes; indeed, the Plateau is crucial to the existence of the East Asian summer rainband (Chen & Bordoni, 2014; Kitoh, 2004). Molnar et al. (2010) argued for a mechanistic effect of the Plateau on the impinging westerlies that produces a downstream stationary eddy circulation that forms the rainband and that the latitudinal migration of the westerlies off the Plateau leads to the latter's demise; this view was subsequently supported in a study by Park et al. (2012). Chiang et al. (2015) followed Molnar et al.'s

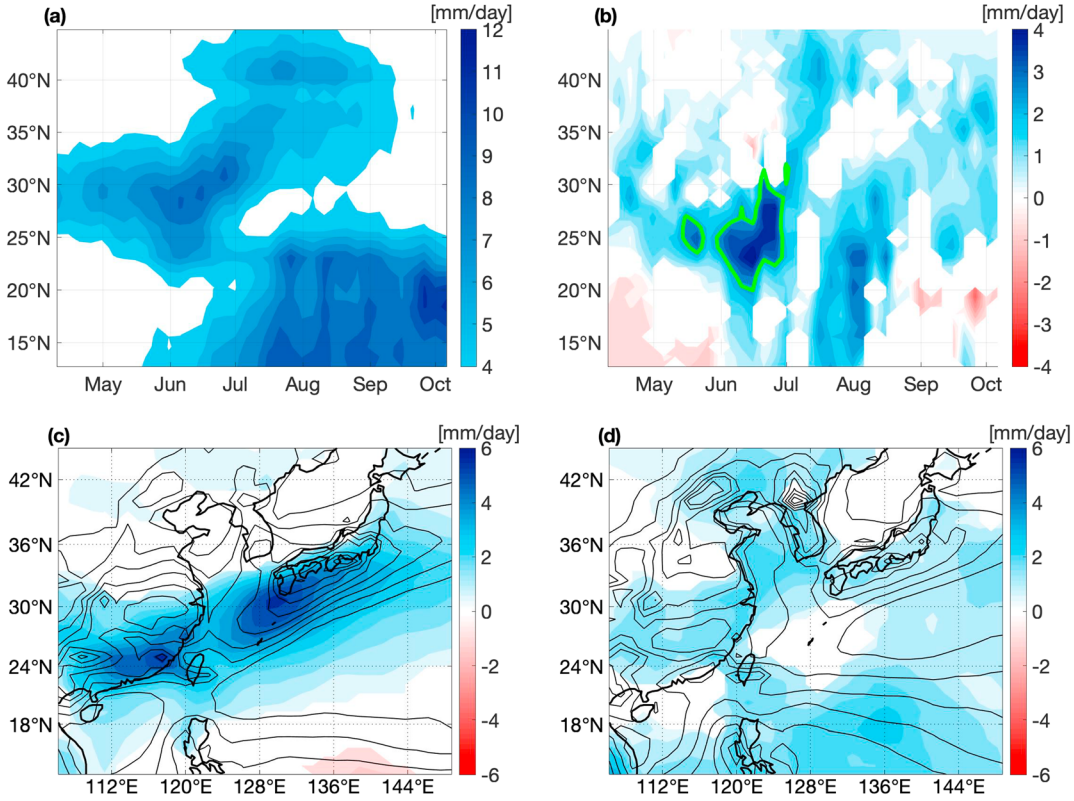

Figure 1. Community Earth System Model version 1 Large Ensemble Project ensemble mean climatological rainfall over East Asia in the early 21st century and changes at the end of the century. (a) Hovmoller of climatological rainfall (early 21st century) for June zonally averaged over East Asia 110°–125°E. (b) Same as (a) but for the difference between the early and late 21st century. Only data that are significant at the 1% level, according to a two-sample *t* test, are shown. Note the marked increase over southeastern China between mid-May and end of June, marked by the green contour which is the 2.5 mm/day contour. (c) Climatological rainfall for June over East Asia (contour interval 1 mm/day, shown are contours between 4 and 12 mm/day) overlaid on top of climatological difference between the early and late 21st century (shading). For the latter, only data that is statistically significant at the 1% level according to a two-sided *t* test is shown. (d) Same as (c) but for July. While rainfall is increased in July, it is spatially diffuse and there is no marked intensification of the rainband.

(2010) lead to propose that changes to the latitudinal migration of the westerlies across the Plateau alter the timing and duration of the East Asian monsoon intraseasonal stages. Subsequent work has lent support to this hypothesis for a range of climate scenarios, including the observed interannual variability (Chiang et al., 2017), changes to Holocene climate (Kong et al., 2017), and last glacial termination (Zhang et al., 2018). These findings beg the question of whether the westerlies play a role in future East Asian rainfall changes.

We explore this question in the context of a pronounced East Asian rainfall response in the Community Earth System Model version 1 Large Ensemble Project (CESM LENS) Representative Control Pathway 8.5 (RCP8.5) simulations (Kay et al., 2015). The late 21st century (2091–2100) shows an early summer rainfall increase (Figures 1b and 1c) and a slight southward displacement of the monsoon rainband, in agreement with Chen and Bordoni (2016). However, the pronounced enhancement occurs only for mid-May through late June, during the pre-Meiyu stage of East Asian rainfall (Figure 1b). The increase is up to 40% of the mean rainfall (Figure 1b), extending over the entire pre-Meiyu rainband (Figure 1c). Extreme rainfall days in June are also enhanced: the number of days where daily rainfall averaged over southeastern China (22°–26°N, 112°–120°E) exceeds 18 mm (approximate at the 90th percentile for the early 21st century, 2006–2015) roughly double by the late 21st century (Figure S1).

This intensification does not occur in the other summer months, and in particular the subsequent Meiyu stage of the intraseasonal sequence in July (Figure 1d). This is surprising, as the pre-Meiyu and Meiyu stage rains possess similar rainband characteristics, with the latter shifted slightly northward relative to the former (Ding & Chan, 2005). The specific timing of the intensification suggests that the underlying cause has to be tied to dynamics that govern East Asian summer monsoon seasonality. Chiang et al. (2015) hypothesized

that the East Asian intraseasonal stage is determined by the meridional position of the westerlies relative to the Plateau. We similarly argue here that the westerlies are the ultimate cause of the simulated pre-Meiyu rainfall enhancement in the CESM LENS simulations. As we will show, the enhancement arises from an intensified meridional circulation downstream of the Plateau resulting in stronger moisture flux convergence over East Asia. This enhancement appears to be a consequence of intensified westerlies impinging on the Tibetan Plateau and consequent modulation of the stationary eddy circulation downstream. The early summer is a time when the late 21st century subtropical jet over Asia is strengthened due to the increased tropical upper tropospheric warming and hence enhanced meridional temperature gradient at the edge of the tropics, coinciding with the latitudes of the Tibetan Plateau.

2. Materials and Methods

We use the CESM LENS (Kay et al., 2015) where the CESM version 1 (Hurrell et al., 2013) model is integrated from 1920 to 2100. Years 1920–2005 use the CMIP5 historical forcing, and years 2006–2100 use the RCP8.5 scenario. The RCP8.5 represents the high-end emissions scenario for the 21st century, with CO_2 concentrations exceeding 900 ppm and radiative forcing reaching 8.5 W/m^2 at the end of the 21st century (Van Vuuren et al., 2011). Each ensemble member is initialized from slightly different atmospheric initial conditions but with the same ocean initialization. Twenty ensemble members are used in our analysis, and only the RCP8.5 (2006–2100) portion. Model fields are vertically interpolated at 30-mb intervals from 30 to 990 mb prior to analysis. The CESM1 has a reasonable simulation of today's East Asian rainfall climatology, in particular its intraseasonal stages (Figures 1a and S2 in the supporting information) and the distinct rainband structure in the early summer (Figure 1c; see also Figure 2 in Horinouchi et al., 2019, that shows the June–July averaged rainfall simulated by various CMIP5 model historical simulations—CESM1 possesses one of the better rainbands in terms of shape and magnitude). In our analysis, we contrast the early 21st century (2006–2015) with the late 21st century (2091–2100) climatology, focusing on monthly means for June and July. In subsequent analysis, "change" refers to the late 21st century climatology minus the early 21st century climatology.

To explore the role of land versus ocean warming in the late 21st century circulation response, we use the CESM1 in an imposed sea surface temperature (SST) configuration where we separately impose the greenhouse gas (GHG) forcing and SST warming for the late 21st century. The F_2000_CAM5 component set is used, which includes the coupler, active atmosphere, land, and sea ice components, and a data ocean model with fixed SST. The atmospheric component of the CESM1 is the Community Atmosphere Model version 5 (CAM5) at 0.9° × 1.25° horizontal resolution with 30 vertical layers. We design four sets of prescribed SST experiments: (1) with the early 21st century SST and GHG concentrations ("early 21stC"), (2) with the late 21st century SST and GHG concentrations ("late 21stC"), (3) with the early 21st century SST and the late 21st century GHG concentrations ("late 21stC GHG"), and (4) with the early 21st century GHG concentrations and the late 21st century SST ("late 21stC SST"). The SST boundary condition for the early 21st century is generated from the midmonth climatology of 20 ensemble members from the CESM LENS (Kay et al., 2015) averaged from 2006 to 2015. Similarly, the SST boundary condition for the late 21st century is generated from the midmonth climatology over 2091–2100. The GHG concentrations for the early and late 21st century simulations are averaged values of corresponding gas concentrations from the CESM Large Ensemble Project over 2006–2015 and 2091–2100, respectively: (early/late 21st century) CO_2 391.92/899.233 ppm, CH_4 1793.32/3712.32 ppb, and N_2O 323.884/429.625 ppb. Each experiment is integrated for 35 years, with the first 5 years treated as spin-up; the climatology derived over the last 30 years is used for the analysis.

3. Moisture Flux Budget Analysis

The vertically integrated moisture budget is analyzed using June monthly mean data to diagnose mechanisms of the pre-Meiyu stage rainfall increase. We follow the same budget treatment in Chen and Bordoni (2016) except that we do not partition specific humidity changes into the temperature and relative humidity components. The monthly mean $P - E$ is related to the vertically integrated horizontal moisture flux divergence as

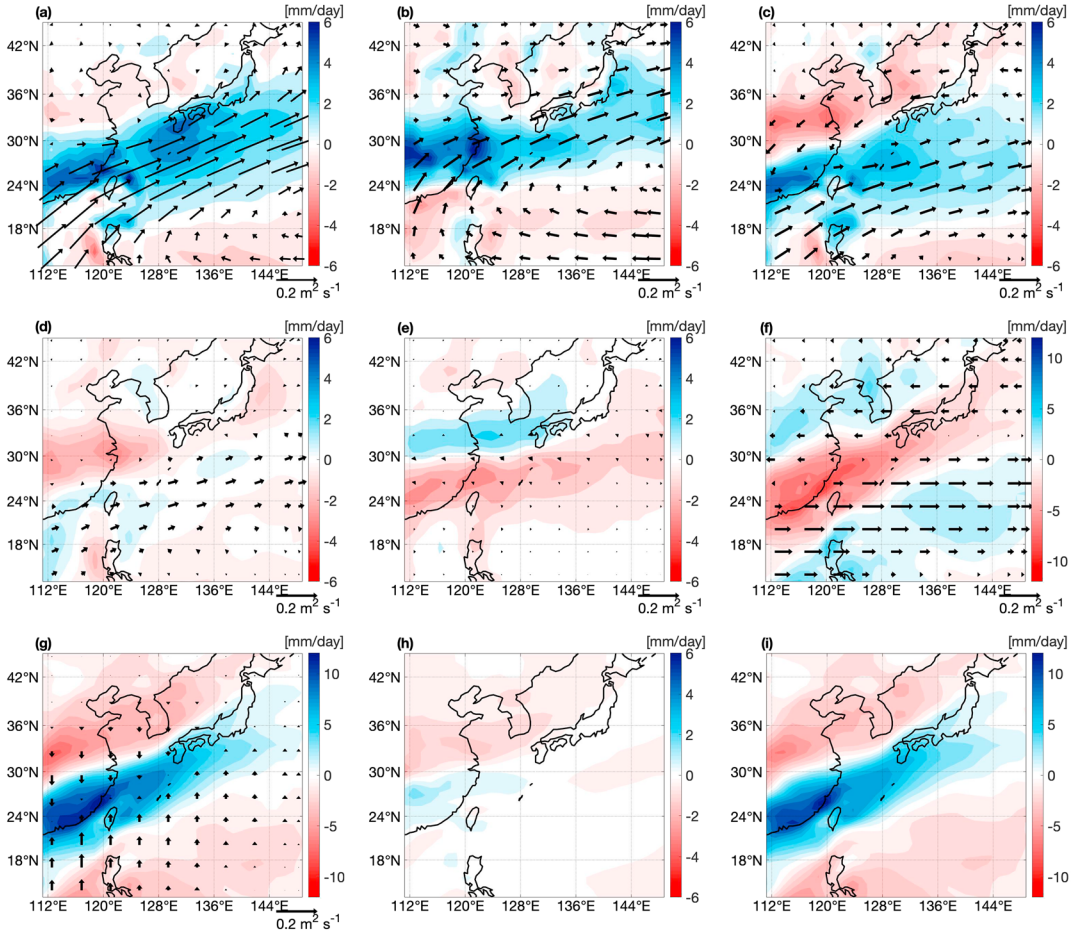

Figure 2. (a–f) Ensemble mean change to the June vertically integrated (surface to 100 mb) components of the moisture budget, late 21st century (2091–2100) minus early 21st century (2006–2015). Moisture flux are shown in vectors, and its convergence is shaded. (a) Moisture flux (qv) and its convergence. (b) Contribution by the change to q. (c) Contribution by change to v. (d) Contribution by change to v and q. (e) Contribution by change to transients. (f) Contribution by change to the zonal wind. (g) Contribution by change to the meridional wind; this term is in turn broken up into contributions by (h) meridional advection of moisture and (i) meridional wind convergence term. Note that the color scale for (f), (g), and (i) span twice the range of the other panels.

$$\overline{P}-\overline{E} = -\left\langle \overline{\nabla.(\vec{v}q)} \right\rangle, \tag{1}$$

where the overbar denotes monthly means, < > indicate the mass-weighted vertical integral from 1000 to 100 mb, and the divergence operator acts only on the horizontal components. The transient contribution to the vertically integrated moisture flux divergence is calculated from monthly mean outputs using

$$tr = \overline{\nabla.(\vec{v}q)} - \left\langle \nabla.\left(\overline{\vec{v}}\,\overline{q}\right) \right\rangle \tag{2}$$

Thus, the change between late 21st century and early 21st century (δ) of equation (1) can be written as (dropping the overbars since we only deal with monthly mean quantities)

$$\underset{\text{(a)}}{\delta(P-E)} = \underset{\text{(a)}}{-\delta\langle\nabla.(\vec{v}q)\rangle} = \underset{\text{(b)}}{-\langle\nabla.(\vec{v}(\delta q))\rangle} \underset{\text{(c)}}{-\langle\nabla.((\delta\vec{v})q)\rangle} \underset{\text{(d)}}{-\langle\nabla.((\delta\vec{v})(\delta q))\rangle} \underset{\text{(e)}}{-\delta(tr)} \tag{3}$$

where the terms on the right-hand side (RHS) are the contributions from (b) the change to the specific humidity, (c) horizontal wind, (d) the cross-perturbation term, and (e) transients, respectively. The pattern and magnitude of change to $P - E$ matches well with the change to the total moisture flux convergence (not shown). The individual terms on the RHS of equation (3) are shown in Figures 2a–2e, respectively; note that (a)–(e) of equation (3) correspond to panels (a)–(e) of Figure 2.

The ensemble mean for June at the end of the 21st century shows increased southwesterly moisture flux leading to increased total moisture flux convergence coincident with the increased $P - E$ (Figure 2a). There is a contribution from the increased specific humidity, consistent with the thermodynamic response to the warming, that leads to an increased moisture flux convergence into central eastern China and the western Pacific (Figure 2b). The increase over eastern China is somewhat north of the $P - E$ increase, but over the ocean the increase is coincident with the $P - E$ increase. This thermodynamic effect on the rainband has been noted before (e.g., Chen & Bordoni, 2016). The contribution from the cross-perturbation term (Figure 2d) is relatively small and largely opposes the contribution from increased specific humidity (Figure 2b).

The interesting component of the budget, however, is the contribution from the change in the horizontal winds (Figure 2c), whose spatial structure largely follows the change in the total moisture flux convergence and in particular over southeastern China. The contribution from the transient changes (Figure 2e) opposes the change from the horizontal winds (Figure 2c), but the magnitude is smaller. Decomposition of the horizontal wind contribution into its zonal and meridional components shows that the convergence over the rainband is entirely due to the flux convergence by the meridional wind (Figure 2g), with the zonal component leading to a compensating drying over the rainband (Figure 2f). Notably, the contribution by the meridional wind has a structure that most resembles the change to the rainfall (Figure 1c).

This pattern of anomalous moisture fluxes by the horizontal circulation change is the consequence of a reduced northward penetration by the low-level circulation. In the climatology, the lower tropospheric southerlies bring moisture from the South China Sea and Western Pacific into southeastern China (Figure S4a). The pattern of low-level wind changes (Figure S4b) indicates a southward shift of this circulation pattern. Our results up to here are consistent with the findings of Chen and Bordoni (2016) insofar as the pattern of precipitation changes is associated with moisture flux convergence induced by the horizontal circulation.

We contrast the June changes with the same analysis but for July. July is primarily during the Meiyu phase of rainfall, and there is a corresponding rainband in the climatology, though northward shifted compared to the pre-Meiyu (compare contours of Figure 1c with that of Figure 1d). While there is a July rainfall increase over the East Asian monsoon region, it is relatively weak and spatially diffuse (Figure 1d). As previously noted, we find it curious that July does not experience a similar rainband intensification, given that the mean rainfall climatology is qualitatively similar to June. The moisture flux budget analysis shows that the July thermodynamic term (Figure S3b) qualitatively exhibits the same behavior as for June—an increase in the northward moisture flux and rainfall somewhat to the north of the rainband—but that the contribution from horizontal wind changes (Figure S3c) and in particular the meridional component (Figure S3g) is considerably smaller. We thus conclude that it is the horizontal wind changes, and specifically the meridional component, that causes the remarkable intensification of the June rainband.

4. Role of the Meridional Circulation Over East Asia

We examine more closely the meridional circulation changes over East Asia. The vertical structure of said changes over June in central China shows increased northerlies throughout the entire depth of the troposphere, suggesting a barotropic midlatitude influence (Figure 3a). An increase in the low-level southerly monsoonal flow is also apparent and mainly over the South China Sea (equatorward of 23°S), only penetrating into the southernmost reaches of southeastern China. The converging flows in the lower and middle troposphere enhance the pre-Meiyu front by bringing warm and moist air from the south to meet with cold dry air from the north; this enhances the lower-tropospheric meridional specific humidity gradient across the climatological position of the pre-Meiyu front, and hence the front itself (Figure 3b). The rainfall intensification occurs around 25°N, south of the front but coinciding with the maximum lower-tropospheric specific humidity change.

The timing of the increase in the midlatitude northerlies coincides exactly with the pre-Meiyu rainfall intensification. The midtropospheric northerly anomalies occur from mid-May through end of June (Figure 3c) and act to enhance the climatological northerlies during that time and extend it slightly further southward; in the neighboring time periods, the anomalous northerlies are absent. Like the midtropospheric anomalies, the lower tropospheric northerly anomalies also occur from mid-May through end of June (Figure 3d),

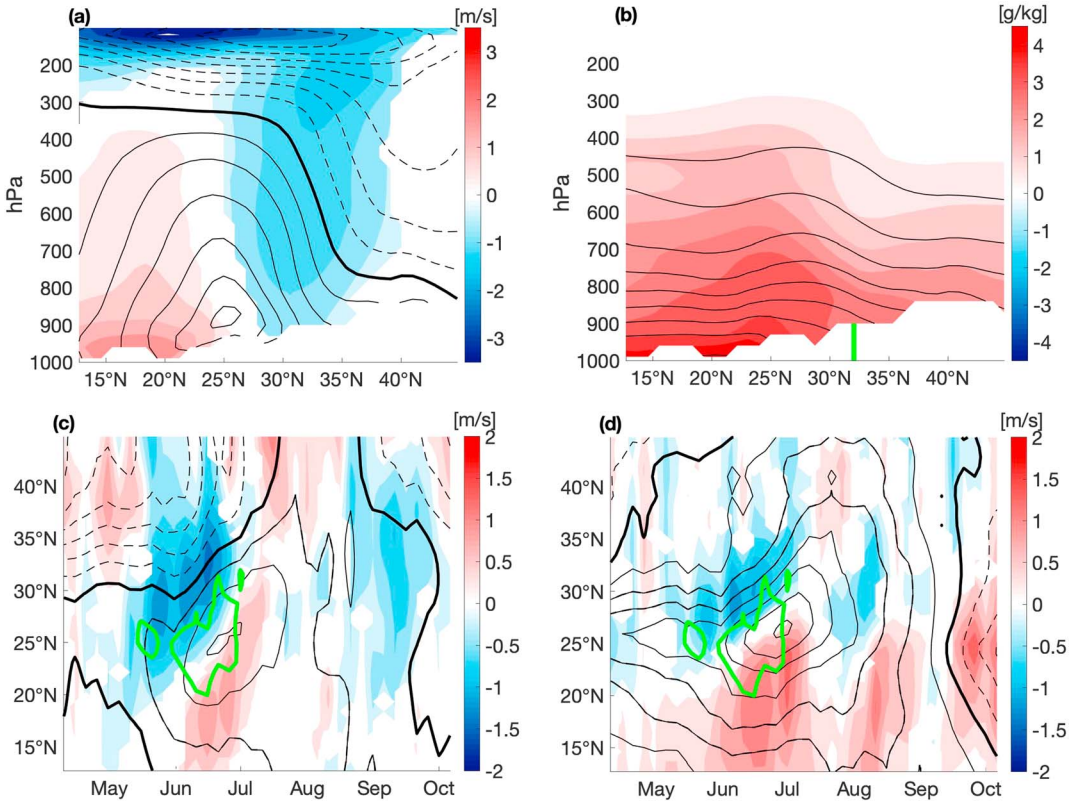

Figure 3. Changes to the meridional flow and pre-Meiyu front, late 21st century (2091–2100) minus early 21st century (2006–2017). (a) Climatological meridional winds (contour interval 1 m/s, thicker line is zero contour) for June and its change at the late 21st century (shaded) zonally averaged between 110° and 125°E. (b) Same as (a) but for specific humidity. Contour interval (in black) is 2 g/kg, and the contour at the very top is 2 g/kg. The green line marks the latitude of the steepest climatological meridional specific humidity gradient at 750 mb, marking the position of the front. (c) Hovmöller of climatological meridional wind at 500 mb zonally averaged over East Asia 110°–125°E (contour interval is 1 m/s, and the thick contour is 0 m/s), overlaid on top of hovmöller of difference between the late 21st and early 21st century (shading). The green contour is the 2.5 mm/day contour as in Figure 1b, showing the rainfall increase over southeastern China. (d) Same as (c) but at 850 mb. In all cases where anomalies are plotted, only data that are statistically significant at the 1% level according to a two-sided *t* test are shown.

indicating a reduced northward penetration of the climatological southerlies; the anomalous northerlies form a barrier to the northward moisture flux. The tropical southerlies to the south of the northerly anomalies also intensify during this time, though the start and end of this intensification occurs later, beginning in early June and ending in early to middle July.

These results, and in particular the concurrent timing between the circulation and rainfall, offer compelling evidence that it is the low-to-middle tropospheric northerlies that initiate the rainfall intensification. There are plausible physical reasons to view the midlatitude northerlies as a causal influence. We break down the meridional moisture flux convergence term (Figure 2g) into its advection (Figure 2h) and wind convergence (Figure 2i) components:

$$\underset{\text{(g)}}{-d_y((\delta v)q)} = \underset{\text{(h)}}{-<\delta v d_y q>} \underset{\text{(i)}}{-<q d_y \delta v>} \tag{4}$$

The advection of cooler and drier air from the north (Figure 2h) steepens the meridional humidity gradient, enhancing the pre-Meiyu front (Figure 3b). Li and Lu (2017) has argued that the presence of cold dry air aloft destabilizes the atmospheric column, promoting moist convection and intensifying rainfall over the Yangtze River Basin. The southward advection of low moist static energy air also explains the slight southward shift of the mean rainband, as the low moist static energy air will limit the northward penetration of the rainfall; this is the so-called "ventilation" mechanism advanced by Chou and Neelin (2003). The intensification can also be viewed as the anomalous convergence of the meridional flow (Figure 2i), which by continuity is the

vertical advection of moisture contributed by the meridional flow. This term explains the bulk of the meridional moisture flux convergence shown in Figure 2g. The anomalous northerlies contribute substantially to the overall wind convergence and thus to the rainband anomaly.

The lower-tropospheric southerly anomalies contribute equally to the moisture flux convergence by the meridional winds (Figure 2g), suggesting that they could cause the rainband intensification, and not the midlatitude northerlies. However, the timing of the enhanced southerlies does not quite match the timing of the rainfall intensification as neatly as for the midtropospheric northerlies (Figure 3d); the southerly anomalies both start and end later, in early June and early to middle July, respectively. The late 21st century shows an almost complete lack of midtropospheric northerly anomalies in July, while there is still some intensification of the tropical lower-tropospheric southerlies (Figure S4d). Rather than being the causal influence, we postulate that the lower-tropospheric southerlies act as a positive feedback on rainfall intensification. By Sverdrup balance ($\beta v \approx f \frac{\partial \omega}{\partial p}$, where v is meridional wind, f is the Coriolis parameter, and β the meridional gradient of f), the southerly flow balances the vortex stretching by the increased diabatic heating (Rodwell & Hoskins, 2001) and in turn brings more moisture to converge over the rainband.

5. Change in the Westerlies Impinging on the Tibetan Plateau

The anomalous midlatitude northerlies possess a barotropic structure, implying that they are produced by midlatitude dynamical processes; in particular, a trough (and associated northerly circulation) directly downstream of the Plateau is a characteristic response of westerlies impinging on large-scale topography (Charney & Eliassen, 1949). Molnar et al. (2010) demonstrated through an idealized atmospheric general circulation model simulation that mechanical forcing on the westerlies by a Plateau-like mountain can generate meridional convergence downstream and heavy rainfall where southeastern China would be located (see their Figure 7). Park et al. (2012) noted that the core westerlies straddle the Plateau in the early summer (April–June) and argued that mechanical forcing by the Plateau on the circulation is responsible for the early summer monsoon rainfall onset over the Bay of Bengal and South China. We thus posit that changes to the westerlies impinging on the Plateau is the cause of the meridional wind changes, and hence the rainfall intensification, at the end of the 21st century.

Indeed, the upper-tropospheric westerlies appear to be intensified over the latitudes of the Plateau and weakened to the north of it (Figure 4a). We examine the temporal behavior of the upper tropospheric westerly anomalies at the western edge of the Plateau (Figure S5). In the early 21stC climatology, the maximum westerlies sit south of the Plateau until early May and then transition to the north of the Plateau by late May (Figure S5a). In the late 21stC, however, the maximum westerlies stay within the latitudes of the Plateau from mid-May through end of June (Figure S5b); this timing coincides with the intensification of the pre-Meiyu rainband.

The question remains as to why the maximum westerlies "linger" over the Plateau latitudes during their northward migration in the late 21st century. Examination of the June tropospheric temperature changes at the latitudes of the Plateau shows a pronounced warming in the tropical mid and upper troposphere extending to around 40°N (Figure 4b, shaded). By thermal wind, the enhanced meridional temperature gradient leads to stronger upper-tropospheric westerlies at the latitudes of the Plateau (Figure 4b, contours). This suggests that the altered westerly circulation originates with the tropical tropospheric thermal response to RCP8.5 forcing.

We examine the separate contributions of the SST warming and the effect of GHG forcing on land warming, using the CESM1 simulations where we separately impose the late 21st century GHG and SST boundary conditions (see section 2). The late 21stC simulation (with late 21st century GHG and SST imposed) shows an anomalous tropospheric temperature and westerly response across the Plateau longitudes that closely resembles that for the late 21st century CESM LENS (figure not shown). The late 21stC GHG simulation (compared to the early 21stC run) shows weaker westerlies across and to the south of the Plateau latitudes, consistent with the warming restricted to the extratropics (Figure 4c). On the other hand, the late 21stC SST run shows a response similar to the CESM1 late 21st century (compare Figure 4d to Figure 4b), but with a more pronounced increase to the westerlies over the Plateau latitudes and to the south. We interpret the stronger westerlies to occur in part because of the lack of enhanced greenhouse warming over the Asian

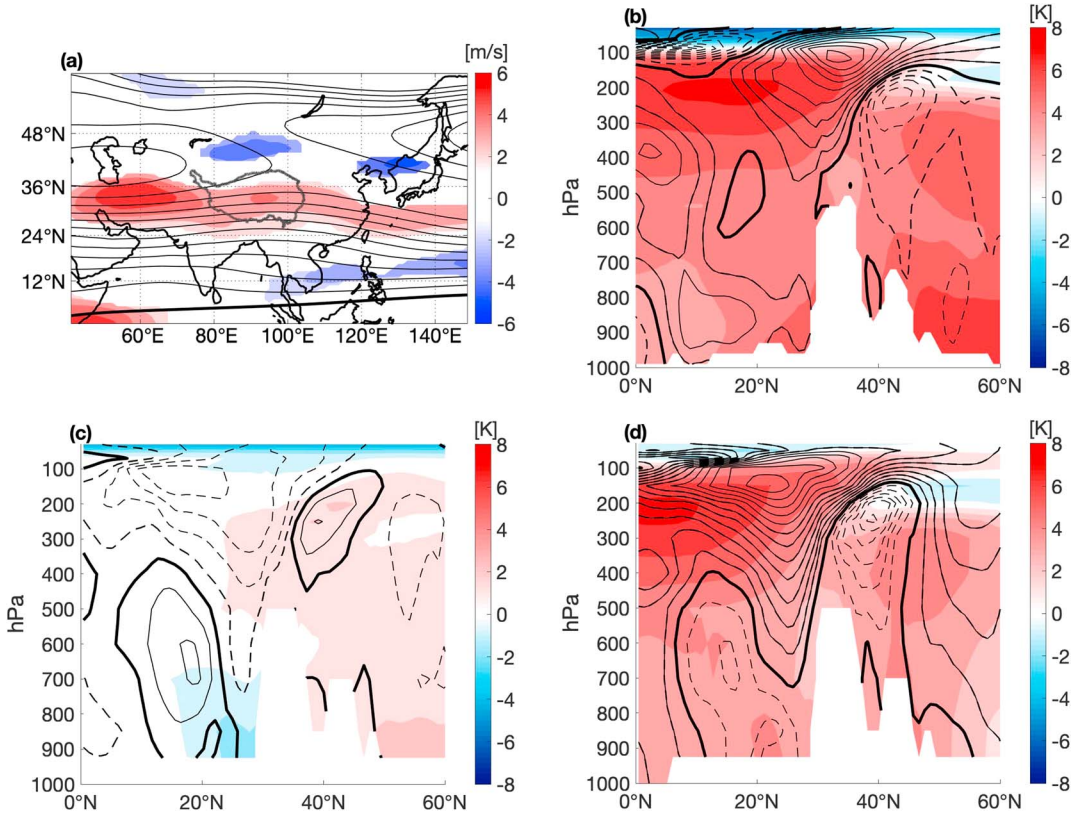

Figure 4. Changes to the westerlies and associated thermal conditions, late 21st century minus early 21st century. (a) Upper tropospheric (210 mb) climatological zonal winds for June over East Asia (contour interval is 3 m/s, with 0 m/s denoted by the thick contour line) overlaid on top of the difference between the early and late 21st century (shading). For the difference, only values significant at the 1% level is shown. An outline of the Tibetan Plateau is shown in grey. (b) Late 21st minus early 21st century change to the June tropospheric temperature (shading, K) at 80°E, at the western edge of the Plateau; overlaid on top of changes to the June zonal winds also at 80°E. (c) Same as (b) but for the difference between the CAM5 late 21stC greenhouse gas and early 21stC simulations, showing the direct contribution from increased greenhouse gases. (d) Same as (b) and (c) but for the difference between the CAM5 late 21stC sea surface temperature and early 21stC simulations, showing the contribution from the altered sea surface temperature. In (b), (c), and (d), the contour interval is 0.5 m/s for the zonal winds (with 0 m/s denoted by the thick contour line) and 1 K for the temperature. Data for the outline of the Plateau in panel (a) are from Zhang et al. (2002).

continental interior in the late 21stC SST run. Thus, the direct effect of greenhouse gases warming the Asian continental interior acts to counter the influence of SST warming on the westerlies over the Plateau latitudes.

The corresponding situation for July is shown in Figure S6. There is still some enhancement of the westerlies over the Plateau latitudes, but it is considerably reduced and also occurs largely north of the Plateau (compare Figure S6a and S6b to Figures 4a and 4b). The late 21stC SST still shows a pronounced tropical upper tropospheric warming and associated enhancement of the westerlies, though the increase is shifted further to the north of the Plateau compared to June (compare Figure S6d to Figure 4d). The larger difference is with the late 21stC GHG run, which shows increased warming in the extratropics in July compared to June, acting to reduce the westerlies over the Plateau latitudes (compare Figure S6c to Figure 4c). The separate effects from SST and GHG forcings lead to a smaller westerly response over the Plateau in July. The CESM-LENS late 21st century westerly changes over the Plateau thus arise from an interplay of the SST-induced tropical tropospheric warming—which is year-round and has little seasonal variation—with the GHG-induced direct warming over the middle- to high-latitude land regions, which is more muted in early summer but increases toward late summer.

6. Conclusions

We find a pronounced enhancement of the East Asian rainband during the pre-Meiyu stage (mid-May to end of June) for the late 21st century in the CESM LENS RCP8.5. The changes result from an intensification of

the meridional stationary eddy circulation occurring downstream of the Tibetan Plateau that enhances the moisture flux convergence into the rainband. We link the meridional stationary eddy changes to an intensification of the westerlies across the Tibetan Plateau, the latter originating from tropical tropospheric warming resulting from warmer tropical ocean surface temperatures that increase the equator-to-pole temperature gradient at the latitudes of the Plateau during the early summer. We note the fortuitous positioning of the Plateau in this response, in that it just happens to span the correct latitudes to interfere with enhanced westerlies resulting from the SST warming.

Our results thus highlight the potential role of the westerlies in altering the East Asian monsoon in the late 21st century. However, we note that our results arise from only one set of model simulations, so the confidence we have of our result to a future global warming climate depends on how reproducible it is with other models. Our purpose here is to argue that the stationary eddy circulation induced by the westerlies impinging on the Tibetan Plateau has a role, and perhaps a dominant one, in East Asian summer rainfall enhancement in the future. A realistic intraseasonal evolution of the simulated East Asian summer monsoon rainfall is necessary to study this phenomenon, since this effect has a distinct intraseasonal character. We do not expect the rainfall enhancement to appear with the exact same timing in other model simulations since the timing of the East Asian monsoon intraseasonal stages differs from model to model. And, averaging different model responses (as one would do in multimodel studies) may have the effect of diluting the rainfall intensification.

Acknowledgments
Model output used here comes from the CESM Large Ensemble Community Project, and supercomputing resources provided by NSF/CISL/Yellowstone. The CESM-LENS data are publicly available from the Earth System Grid, https://www.earthsystemgrid.org/home.html. For CESM-fixed SST simulations, we acknowledge high-performance computing support from Cheyenne (https://doi.org/10.5065/D6RX99HX) provided by NCAR's Computational and Information Systems Laboratory, sponsored by the National Science Foundation. Model output for the CESM fixed SST simulations is archived and available at http:// https://doi.org/10.6078/D12099 (Chiang et al., 2019). We thank Inez Fung for her input and helpful discussion on this work. This work was supported by the Department of Energy grant DE-SC0014078 and National Science Foundation grant AGS-1405479.

References

Charney, J. G., & Eliassen, A. (1949). A numerical method for predicting the perturbations of the middle latitude westerlies. *Tellus*, *1*(2), 38–54. https://doi.org/10.1111/j.2153-3490.1949.tb01258.x

Chen, J., & Bordoni, S. (2014). Orographic effects of the Tibetan Plateau on the East Asian Summer Monsoon: An energetic perspective. *Journal of Climate*, *27*, 3052–3072. https://doi.org/10.1175/jcli-d-13-00479

Chen, J., & Bordoni, S. (2016). Early summer response of the East Asian summer monsoon to atmospheric CO_2 forcing and subsequent sea surface warming. *Journal of Climate*, *29*(15), 5431–5446. https://doi.org/10.1175/JCLI-D-15-0649.1

Chiang, J., Swenson, L., & Kong, W. (2017). Role of seasonal transitions and the westerlies in the interannual variability of the East Asian summer monsoon precipitation. *Geophysical Research Letters*, *44*, 3788–3795. https://doi.org/10.1002/2017GL072739

Chiang, J. C. H., Fung, I. Y., Wu, C. H., Cai, Y. H., Edman, J. P., Liu, Y. W., et al. (2015). Role of seasonal transitions and westerly jets in East Asian paleoclimate. *Quaternary Science Reviews*, *108*, 111–129. https://doi.org/10.1016/j.quascirev.2014.11.009

Chiang, J., Fischer, J., Kong, W., Herman, M. (2019). Forcing files and model output for "Intensification of the pre-Meiyu rainband in the late 21st century", UC Berkeley Dash, Dataset. https://doi.org/10.6078/D12099

Chou, C., & Neelin, J. D. (2003). Mechanisms limiting the northward extent of the northern summer monsoons over North America, Asia, and Africa. *Journal of Climate*, *16*(3), 406–425. https://doi.org/10.1175/1520-0442(2003)016<0406:MLTNEO>2.0.CO;2

Ding, Y., & Chan, J. C. L. (2005). The East Asian summer monsoon: An overview. *Meteorology and Atmospheric Physics*, *89*(1-4), 117–142. https://doi.org/10.1007/s00703-005-0125-z

Held, I. M., & Soden, B. J. (2006). Robust responses of the hydrological cycle to global warming. *Journal of Climate*, *19*(21), 5686–5699. https://doi.org/10.1175/JCLI3990.1

Horinouchi, T., Matsumura, S., Ose, T., & Takayabu, Y. N. (2019). Jet-precipitation relation and future change of mei-yu/baiu rainband and subtropical jet in CMIP5 coupled GCM simulations. *Journal of Climate*, *32*, 2247–2259. https://doi.org/10.1175/JCLI-D-18-0426.1

Hurrell, J. W., Holland, M. M., Gent, P. R., Ghan, S., Kay, J. E., Kushner, P. J., et al. (2013). The Community Earth System Model: A framework for collaborative research. *Bulletin of the American Meteorological Society*, *94*(9), 1339–1360. https://doi.org/10.1175/BAMS-D-12-00121.1

Kamae, Y., Watanabe, M., Kimoto, M., & Shiogama, H. (2014). Summertime land–sea thermal contrast and atmospheric circulation over East Asia in a warming climate—Part I: Past changes and future projections. *Climate Dynamics*, *43*(9-10), 2553–2568. https://doi.org/10.1007/s00382-014-2073-0

Kay, J., Deser, C., Phillips, A., Mai, A., Hannay, C., Strand, G., et al. (2015). The Community Earth System Model (CESM) large ensemble project: A community resource for studying climate change in the presence of internal climate variability. *Bulletin of the American Meteorological Society*, *96*(8), 1333–1349. https://doi.org/10.1175/BAMS-D-13-00255.1

Kitoh, A. (2004). Effects of mountain uplift on East Asian summer climate investigated by a coupled atmosphere-ocean GCM. *Journal of Climate*, *17*(4), 783–802. https://doi.org/10.1175/1520-0442(2004)017<0783:Eomuoe>2.0.Co;2

Kitoh, A., Endo, H., Kumar, K. K., Cavalcanti, I. F., Goswami, P., & Zhou, T. (2013). Monsoons in a changing world: A regional perspective in a global context. *Journal of Geophysical Research: Atmospheres*, *118*, 3053–3065. https://doi.org/10.1002/jgrd.50258

Kong, W., Swenson, L. M., & Chiang, J. C. (2017). Seasonal transitions and the westerly jet in the Holocene East Asian summer monsoon. *Journal of Climate*, *30*(9), 3343–3365. https://doi.org/10.1175/JCLI-D-16-0087.1

Li, X., & Lu, R. (2017). Extratropical factors affecting the variability in summer precipitation over the Yangtze River basin, China. *Journal of Climate*, *30*(20), 8357–8374. https://doi.org/10.1175/JCLI-D-16-0282.1

Molnar, P., Boos, W. R., & Battisti, D. S. (2010). Orographic controls on climate and paleoclimate of Asia: Thermal and mechanical roles for the Tibetan Plateau. *Annual Review of Earth and Planetary Sciences*, *38*(1), 77–102. https://doi.org/10.1146/annurev-earth-040809-152456

Park, H. S., Chiang, J. C. H., & Bordoni, S. (2012). The mechanical impact of the Tibetan Plateau on the seasonal evolution of the South Asian monsoon. *Journal of Climate*, *25*(7), 2394–2407. https://doi.org/10.1175/JCLI-D-11-00281.1

Rodwell, M. J., & Hoskins, B. J. (2001). Subtropical anticyclones and summer monsoons. *Journal of Climate*, *14*(15), 3192–3211. https://doi.org/10.1175/1520-0442(2001)014<3192:SAASM>2.0.CO;2

Shaw, T., & Voigt, A. (2015). Tug of war on summertime circulation between radiative forcing and sea surface warming. *Nature Geoscience*, *8*(7), 560–566. https://doi.org/10.1038/ngeo2449

Van Vuuren, D. P., Edmonds, J., Kainuma, M., Riahi, K., Thomson, A., Hibbard, K., et al. (2011). The representative concentration pathways: an overview. *Climate Change*, *109*(1-2), 5. https://doi.org/10.1007/s10584-011-0148

Zhang, H., Griffiths, M. L., Chiang, J. C., Kong, W., Wu, S., Atwood, A., et al. (2018). East Asian hydroclimate modulated by the position of the westerlies during Termination I. *Science*, *362*(6414), 580–583. https://doi.org/10.1126/science.aat9393

Zhang, Y., Li, B., & Zheng, D. (2002). Datasets of the boundary and area of the Tibetan Plateau. Global Change Research Data Publishing and Repository, 2014. DOI:10.3974/geodb.2014.01. 12. v1.

Zou, L. W., & Zhou, T. J. (2013). Near future (2016-40) summer precipitation changes over China as projected by a regional climate model (RCM) under the RCP8.5 emissions scenario: Comparison between RCM downscaling and the driving GCM. *Advances in Atmospheric Sciences*, *30*(3), 806–818. https://doi.org/10.1007/s00376-013-2209-x

References From the Supporting Information

Yatagai, A., Arakawa, O., Kamiguchi, K., Kawamoto, H., Nodzu, M. I., & Hamada, A. (2009). A 44-year daily gridded precipitation dataset for Asia based on a dense network of rain gauges. *Sola*, *5*, 137–140. https://doi.org/10.2151/sola.2009-035